Local versus global buckling of thin films on elastomeric substrates

Shuodao Wang,[1] Jizhou Song,[2] Dae-Hyeong Kim,[3] Yonggang Huang,[1,4,a)] and John A. Rogers[2,3,5,a)]
[1]*Department of Mechanical Engineering, Northwestern University, Evanston, Illinois 60208, USA*
[2]*Department of Mechanical Science and Engineering, University of Illinois at Urbana-Champaign, Illinois 61801, USA*
[3]*Department of Materials Science and Engineering, Beckman Institute, and Frederick Seitz Materials Research Laboratory, University of Illinois at Urbana-Champaign, Urbana, Illinois 61801, USA*
[4]*Department of Civil and Environmental Engineering, Northwestern University, Evanston, Illinois 60208, USA*
[5]*Department of Chemistry, University of Illinois at Urbana-Champaign, Urbana, Illinois 61801, USA*

(Received 20 May 2008; accepted 18 June 2008; published online 17 July 2008)

Local buckling can form microcorrugations in thin films on elastomeric substrates, to yield an effective type of mechanical stretchability in otherwise rigid, brittle materials, with many application possibilities. For large area films or relatively thin substrates, however, global (Euler) buckling, as opposed to local buckling, can be observed in experiments. This paper describes analytically the mechanics of local and global buckling of one-dimensional thin films or two-dimensional thin membranes on elastomeric substrates. The critical condition separating these two buckling modes is obtained analytically, and it agrees well with experiments and numerical simulations. © *2008 American Institute of Physics*. [DOI: 10.1063/1.2956402]

Thin films on elastomeric substrates are important for electronics systems that require or benefit from mechanical stretchability, such as flexible displays,[1] electronic eye camera,[2] conformable skin sensors,[3] smart surgical gloves,[4] and structural health monitoring devices.[5] Other emerging applications include micro- and nanoelectromechanical systems,[6] tunable phase optics,[7,8] force spectroscopy in cells,[9] biocompatible topographic matrices for cell alignment,[10,11] high precision micro- and nanometrology methods,[12–15] and pattern formation for micro- and nanofabrication.[16–22] Figures 1(a) and 1(b) schematically illustrate one method for integrating thin films of high quality electronic materials (e.g., silicon) with elastomeric substrates for stretchable electronics.[23–26] Thin ribbons of single crystal silicon are bonded to flat, prestrained elastomeric substrates of poly(dimethylsiloxane) (PDMS) [Fig. 1(a)]. The release of prestrain leads to compressive strains in the ribbons that generate the local buckling pattern [Fig. 1(b)].

Early mechanics models[23,27,28] give the wavelength $\lambda_0 = \pi h_f / \sqrt{\varepsilon_{\text{critical}}^{\text{local}}}$ and amplitude $A_0 = h_f \sqrt{\varepsilon_{\text{pre}} / \varepsilon_{\text{critical}}^{\text{local}} - 1}$ of the local buckling profile (inset of Fig. 2), which are both proportional to the film thickness h_f, the amplitude increases with the prestrain, and

$$\varepsilon_{\text{critical}}^{\text{local}} = \frac{1}{4}\left(\frac{3\bar{E}_s}{\bar{E}_f}\right)^{2/3} \tag{1}$$

is the critical buckling strain given in terms of the plane-strain elastic moduli $\bar{E}_f$ and $\bar{E}_s$ of the film and substrate. The wavelength and amplitude agree well with experiments,[23] and have been used as in modern metrology.[12–15] The substrate thickness h_s does not come into play because the substrate is much thicker than the film and therefore is considered as a semi-infinite solid.

Another buckling mode, namely, the global buckling shown in Fig. 1(c), has been observed in experiments for cases where the substrate is relatively thin. Although this behavior can be eliminated by adding thin layers of substrate material on top of the system,[29] an understanding of the physics is important for this emerging field of technology. The objective of this letter is to identify the critical condition separating the local and global buckling modes for an elastic film on an elastomeric substrate. The critical strain for global buckling $\varepsilon_{\text{critical}}^{\text{global}}$, to be given in the following, is compared to the local buckling strain $\varepsilon_{\text{critical}}^{\text{local}}$ in Eq. (1) to determine the critical condition separating the two buckling modes.

The film and substrate are modeled as a composite beam in global buckling. The effective tensile rigidity of the composite beam is $\overline{EA} = \bar{E}_s h_s + \bar{E}_f h_f$, while the effective bending rigidity is[30] $\overline{EI} = \dfrac{(\bar{E}_f h_f^2 - \bar{E}_s h_s^2)^2 + 4\bar{E}_f h_f \bar{E}_s h_s (h_f + h_s)^2}{12(\bar{E}_f h_f + \bar{E}_s h_s)}$. The

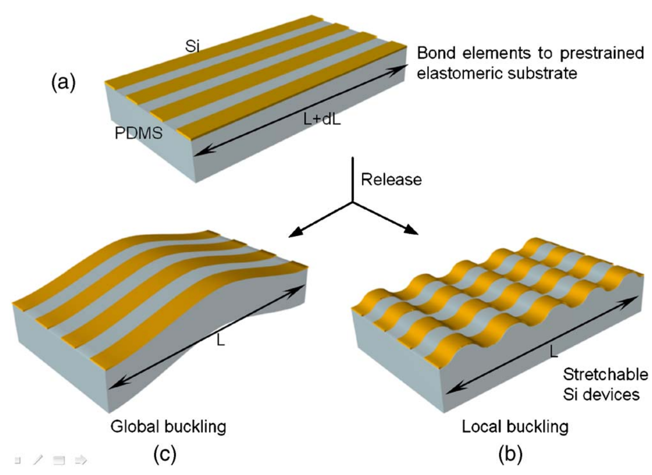

FIG. 1. (Color online) Schematic illustration of the process for fabricating buckled single crystal Si ribbons (yellow) on a PDMS (gray) substrate; (a) bond Si elements to prestretched PDMS; (b) local buckling; and (c) global buckling due to release of prestretch.

a)Authors to whom correspondence should be addressed. Electronic addresses: y-huang@northwestern.edu and jrogers@uiuc.edu.

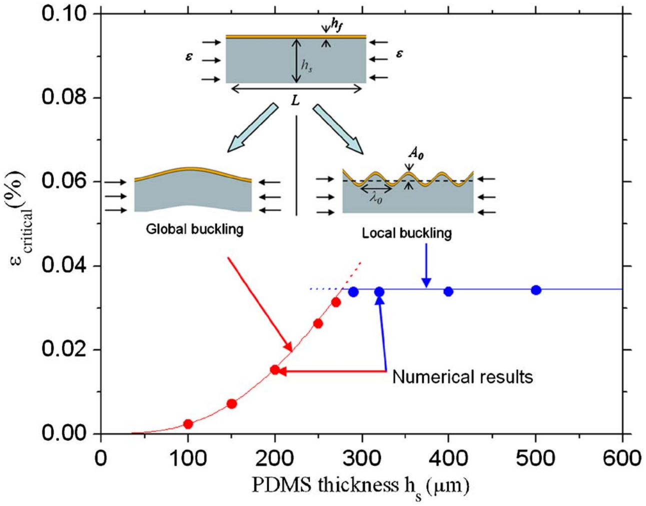

FIG. 2. (Color online) Critical strains of one-dimensional local and global bucklings vs substrate thickness h_s for the Si/PDMS system.

critical buckling strain for a beam of length L with clamped ends, accounting for the shear effect, is[31]

$$\varepsilon_{\text{critical}}^{\text{global}} = \frac{1}{1 + \dfrac{1.2F_{\text{cr}}^0}{\overline{G}(h_s + h_f)}} \frac{F_{\text{cr}}^0}{\overline{EA}} \tag{2}$$

for a rectangular cross section, where $F_{\text{cr}}^0 = 4\pi^2\overline{EI}/L^2$ is the critical buckling load neglecting the effect of shear, and $\overline{G}$ is the effective shear modulus of the composite beam, which is approximately the shear modulus G_s of the substrate since the film is very stiff ($E_f \gg E_s$) and thin ($h_f \ll h_s$).

Local buckling occurs when its critical strain in Eq. (1) is smaller than its counterpart in Eq. (2) for global buckling, i.e., $\varepsilon_{\text{critical}}^{\text{local}} < \varepsilon_{\text{critical}}^{\text{global}}$, while global buckling occurs when the opposite holds, $\varepsilon_{\text{critical}}^{\text{local}} > \varepsilon_{\text{critical}}^{\text{global}}$. This is equivalent to comparing the energy in local and global buckling. Figure 2 shows the critical local and global buckling strains versus the substrate thickness h_s for a 1-μm-thick, 3-mm-long Si film (Young's modulus $E_f = 130$ GPa, Poisson's ratio $\nu_f = 0.27$) (Ref. 32) on a PDMS substrate ($E_s = 1.8$ MPa, $\nu_s = 0.5$).[15] The global buckling strain (red curve) increases with the substrate thickness, while the local buckling strain remains a constant, ~0.034% (blue line). For small substrate thickness such that $\varepsilon_{\text{critical}}^{\text{local}} > \varepsilon_{\text{critical}}^{\text{global}}$, global buckling occurs, while local buckling

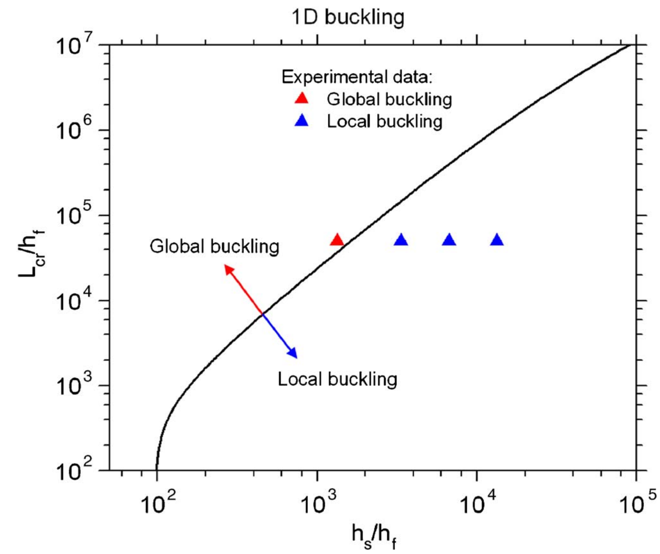

FIG. 3. (Color online) Critical condition of one-dimensional local and global bucklings for the Si/PDMS system.

occurs for a thick substrate. The condition $\varepsilon_{\text{critical}}^{\text{local}} = \varepsilon_{\text{critical}}^{\text{global}}$, which corresponds to the intercept of two curves in Fig. 2, gives a critical length L_{cr} separating local and global bucking as

$$L_{\text{cr}} = 4\pi\sqrt{\overline{EI}\left\{\frac{[\overline{E}_f/(3\overline{E}_s)]^{2/3}}{\overline{E}_s h_s + \overline{E}_f h_f} - \frac{0.3}{G_s(h_f + h_s)}\right\}}. \tag{3}$$

Local and global buckling occur for $L < L_{\text{cr}}$ and $L > L_{\text{cr}}$, respectively.

The finite element method is used to verify the above criterion for local and global bucklings. Beam elements are used for the film, while the substrate is modeled by solid elements. The numerical results are shown in Fig. 2 (blue dots for local buckling and red dots for global buckling), and they agree very well with the analytical expressions (1) and (2).

Figure 3 shows the critical length normalized by film thickness, L_{cr}/h_f, versus the ratio of substrate to film thickness, h_s/h_f, for the Si film on PDMS substrate. This curve separates local buckling (below the curve) from global buckling (above the curve). Experimental results (solid circles) are also shown in Fig. 3 for film thickness $h_f = 300$ nm,

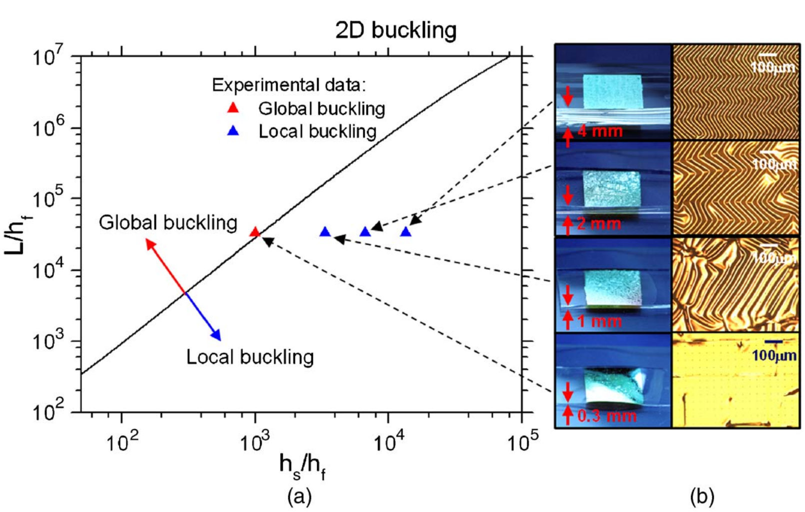

FIG. 4. (Color online) (a) Critical condition and (b) optical images of two-dimensional local and global bucklings for the Si/PDMS system.

length $L=15$ mm, and several substrate thickness $h_s=0.4$, 0.6, 1.0, 2.0, and 4.0 mm. Local buckling is observed for all substrate thickness except for $h_s=0.4$ mm, for which global buckling occurs. For $h_f=300$ nm and $L=15$ mm as in experiments, Fig. 3 gives a critical substrate thickness $h_s=0.51$ mm separating the local and global buckling. This agrees very well with the experiments, $h_s=0.4$ mm for global buckling and 0.6, 1.0, 2.0, and 4.0 mm for local buckling.

Local and global bucklings are also observed in two-dimensional Si thin membrane on PDMS substrate subject to equibiaxial compression. Thin single crystal silicon membranes were prepared from silicon on insulator wafer [Soitec, Unibond; Si (300 nm)/SiO_2 (1000 nm)] and covalently bonded to various thickness PDMS, where the bonding was promoted by the UV/ozone treatment.[33] The optical images in Fig. 4(b) show local buckling for membrane thickness $h_s=1.0$, 2.0, and 4.0 mm, and global buckling for $h_s=0.3$ mm. The Si membrane has length and width $L_1\times L_2=10.4\times 10.4\ \mathrm{mm}^2$, and thickness $h_f=300$ nm. The critical strain for local buckling is $(\varepsilon_{\mathrm{critical}}^{\mathrm{local}})^{2D}=(3\bar{E}_s/\bar{E}_f)^{2/3}/[4(1+\nu_f)]$.[26,34] For global buckling, the film and substrate are modeled as a composite plate with dimensions $L_1\times L_2$, effective tensile rigidity $\overline{EA}$, and bending rigidity $\overline{EI}$. These give the critical strain for global buckling $(\varepsilon_{\mathrm{critical}}^{\mathrm{global}})^{2D}=\left[\frac{4(1-\nu_s)\pi^2\overline{EI}}{\overline{EA}}\right]\left(\frac{1}{L_1^2}+\frac{1}{L_2^2}\right)$.[35] The critical length L_{cr} $(=L_1=L_2)$ separating local and global buckling is determined from $(\varepsilon_{\mathrm{critical}}^{\mathrm{local}})^{2D}=(\varepsilon_{\mathrm{critical}}^{\mathrm{global}})^{2D}$, and is shown versus the ratio of substrate to membrane thickness, h_s/h_f, in Fig. 4(a). For $h_f=300$ nm and $L_1=L_2=10.4$ mm as in experiments, Fig. 4(a) gives a critical substrate thickness $h_s=0.35$ mm below which global buckling occurs. This agrees very well with the experimental images in Fig. 4(b), which show global buckling for $h_s=0.3$ mm and local buckling $h_s=1.0$, 2.0, and 4.0 mm [also shown by solid triangles in Fig. 4(a)].

In summary, the critical condition for local and global buckling of thin films on compliant substrates is obtained analytically, and it agrees well with experimental and numerical results.

The authors acknowledge the support from the National Science Foundation (DMI-0328162), and the U.S. Department of Energy, Division of Materials Sciences (DEFG02-91ER45439).

[1] G. P. Crawford, Flexible Flat Panel Display Technology (Wiley, New York, 2005).
[2] H. C. Ko, M. P. Stoykovich, J. Song, V. Malyarchuk, W. M. Choi, C.-J. Yu, J. B. Geddes, J. Xiao, S. Wang, Y. Huang, and J. A. Rogers, "A hemispherical electronic eye camera based on compressible silicon optoelectronics," Nature (in press).
[3] V. Lumelsky, M. S. Shur, and S Wagner, IEEE Sens. J. **1**, 41 (2001).
[4] T. Someya, T. Sekitani, S. Iba, Y. Kato, H. Kawaguchi, and T. Sakurai, Proc. Natl. Acad. Sci. U.S.A. **101**, 9966 (2004).
[5] A. Nathan, B. Park, A. Sazonov, S. Tao, I. Chan, P. Servati, K. Karim, T. Charania, D. Striakhilev, Q. Ma, and R. V. R. Mruthy, Microelectron. J. **31**, 883 (2000).
[6] Y. Q. Fu, S. Sanjabi, Z. H. Barber, T. W. Clyne, W. M. Huang, M. Cai, J. K. Luo, A. J. Flewitt, and W. I. Milne, Appl. Phys. Lett. **89**, 3 (2006).
[7] C. Harrison, C. M. Stafford, W. H. Zhang, and A. Karim, Appl. Phys. Lett. **85**, 4016 (2004).
[8] K. Efimenko, M. Rackaitis, E. Manias, A. Vaziri, L. Mahadevan, and J. Genzer, Nat. Mater. **4**, 293 (2005).
[9] A. K. Harris, P. Wild, and D. Stopak, Science **208**, 177 (1980).
[10] A. I. Teixeira, G. A. Abrams, P. J. Bertics, C. J. Murphy, and P. F. Nealey, J. Cell. Sci. **116**, 1881 (2003).
[11] X. Y. Jiang, S. Takayama, X. P. Qian, E. Ostuni, H. K. Wu, N. Bowden, P. LeDuc, D. E. Ingber, and G. M. Whitesides, Langmuir **18**, 3273 (2002).
[12] C. M. Stafford, S. Guo, C. Harrison, and M. Y. M. Chiang, Rev. Sci. Instrum. **76**, 5 (2005).
[13] C. M. Stafford, C. Harrison, K. L. Beers, A. Karim, E. J. Amis, M. R. Vanlandingham, H. C. Kim, W. Volksen, R. D. Miller, and E. E. Simonyi, Nat. Mater. **3**, 545 (2004).
[14] C. M. Stafford, B. D. Vogt, C. Harrison, D. Julthongpiput, and R. Huang, Macromolecules **39**, 5095 (2006).
[15] E. A. Wilder, S. Guo, S. Lin-Gibson, M. J. Fasolka, and C. M. Stafford, Macromolecules **39**, 4138 (2006).
[16] N. Bowden, S. Brittain, A. G. Evans, J. W. Hutchinson, and G. M. Whitesides, Nature (London) **393**, 146 (1998).
[17] N. Bowden, W. T. S. Huck, K. E. Paul, and G. M. Whitesides, Appl. Phys. Lett. **75**, 2557 (1999).
[18] W. T. S. Huck, N. Bowden, P. Onck, T. Pardoen, J. W. Hutchinson, and G. M. Whitesides, Langmuir **16**, 3497 (2000).
[19] J. S. Sharp and R. A. L. Jones, Adv. Mater. (Weinheim, Ger.) **14**, 799 (2002).
[20] P. J. Yoo, K. Y. Suh, S. Y. Park, and H. H. Lee, Adv. Mater. (Weinheim, Ger.) **14**, 1383 (2002).
[21] H. Schmid, H. Wolf, R. Allenspach, H. Riel, S. Karg, B. Michel, and E. Delamarche, Adv. Funct. Mater. **13**, 145 (2003).
[22] M.-W. Moon, S. H. Lee, J.-Y. Sun, K. H. Oh, A. Vaziri, and J. W. Hutchinson, Proc. Natl. Acad. Sci. U.S.A. **104**, 1130 (2007).
[23] D. Y. Khang, H. Jiang, Y. Huang, and J. A. Rogers, Science **311**, 208 (2006).
[24] H. Jiang, D. Y. Khang, J. Song, Y. Sun, Y. Huang, and J. A. Rogers, Proc. Natl. Acad. Sci. U.S.A. **104**, 15607 (2007).
[25] J. Song, H. Jiang, Z. J. Liu, D. Y. Khang, Y. Huang, J. A. Rogers, C. Lu, and C. G. Koh, Int. J. Solids Struct. **45**, 3107 (2008).
[26] C. T. Koh, Z. J. Liu, D. Y. Khang, J. Song, C. Lu, Y. Huang, J. A. Rogers, and C. G. Koh, Appl. Phys. Lett. **91**, 133113 (2007).
[27] X. Chen and J. W. Hutchinson, J. Appl. Mech. **71**, 597 (2004).
[28] Z. Y. Huang, W. Hong, and Z. Suo, J. Mech. Phys. Solids **53**, 2101 (2005).
[29] D. H. Kim, J. H. Ahn, W. M. Choi, H. S. Kim, T. H. Kim, J. Song, Y. Huang, Z. J. Liu, C. Lu, and J. A. Rogers, Science **320**, 507 (2008).
[30] D. Gray, S. V. Hoa, and S. W. Tsai, *Composite Materials: Design and Applications* (CRC, Boca Raton, FL, 2003), Chap. 13, pp. 283–385.
[31] Z. P. Bazant and L. Cedolin, *Stability of Structures* (Dover, New York, 2003), Chap. 1, pp. 31–32.
[32] INSPEC, *Properties of Silicon* (Institution of Electrical Engineers, New York, 1998).
[33] W. M. Choi, J. Song, D.-Y. Khang, H. Jiang, Y. Huang, and J. A. Rogers, Nano Lett. **7**, 1655 (2007).
[34] J. Song, H. Jiang, W. M. Choi, D. Y. Khang, Y. Huang, and J. A. Rogers, J. Appl. Phys. **103**, 014303 (2008).
[35] S. P. Timoshenko and J. M. Gere, *Theory of Elastic Stability* (McGraw-Hill, New York, 1961).